Circulation
Cardiovascular Interventions
JOURNAL OF THE AMERICAN HEART ASSOCIATION
American Heart Association
Learn and Live

Predictors of Periprocedural (Type IVa) Myocardial Infarction, as Assessed by Frequency-Domain Optical Coherence Tomography

Italo Porto, Luca Di Vito, Francesco Burzotta, Giampaolo Niccoli, Carlo Trani, Antonio M. Leone, Luigi M. Biasucci, Rocco Vergallo, Ugo Limbruno and Filippo Crea

Circ Cardiovasc Interv published online January 31, 2012;
DOI: 10.1161/CIRCINTERVENTIONS.111.965624
Circulation: Cardiovascular Interventions is published by the American Heart Association. 7272 Greenville Avenue, Dallas, TX 72514
 Print ISSN: 1941-7640. Online ISSN: 1941-7632

Predictors of Periprocedural (Type IVa) Myocardial Infarction, as Assessed by Frequency-Domain Optical Coherence Tomography

Italo Porto, MD, PhD; Luca Di Vito, MD; Francesco Burzotta, MD, PhD; Giampaolo Niccoli, MD, PhD; Carlo Trani, MD, PhD; Antonio M. Leone, MD, PhD; Luigi M. Biasucci, MD, PhD; Rocco Vergallo, MD; Ugo Limbruno, MD; Filippo Crea, MD, FESC

Background—Frequency-domain optical coherence tomography (FD-OCT) is easily able to define both pre- and post-stenting features of the atherosclerotic plaque that can potentially be related to periprocedural complications. We sought to examine which FD-OCT-defined characteristics, assessed both before and after stent deployment, predicted periprocedural (type IVa) myocardial infarction (MI).

Methods and Results—FD-OCT was performed before and after coronary stenting in 50 patients undergoing percutaneous coronary intervention (PCI) for either non-ST segment elevation MI (NSTEMI) or stable angina. All patients underwent single-vessel stenting, and only drug-eluting stents were implanted. Troponin T was analyzed on admission, before PCI, and at 12 and 24 hours after PCI, and type IVa MI was defined in stable angina as a rise of at least 3× upper reference limit and in NSTEMI as a pre-PCI troponin T fall, followed by post-PCI troponin T rise >20%. Type IVa MI was diagnosed in 21 patients, while the remaining 29 represented the control group. FD-OCT analysis showed that thin-cap fibroatheroma (76.2% versus 41.4%; $P=0.017$) prior to PCI, intrastent thrombus (61.9% versus 20.7%; $P=0.04$), and intrastent dissection (61.9% versus 31%; $P=0.03$) after PCI were significantly more frequent in type IVa MI than in the control group. Multivariate logistic regression analysis confirmed thin-cap fibroatheroma (OR 29.7, 95% CI 1.4 to 32.1), intrastent thrombus (OR 5.5, CI 1.2 to 24.9) and intrastent dissection (OR 5.3, CI 1.2 to 24.3) as independent predictors of type IVa MI.

Conclusions—In conclusion, presence of thin-cap fibroatheroma at pre-PCI FD-OCT and of intrastent thrombus and intrastent dissection at post-PCI FD-OCT predict type IVa MI in a contemporary sample of patients treated with second-generation drug-eluting stents. Interestingly, 2 of the 3 predictors of type IVa MI were not apparent at pre-PCI FD-OCT. **(*Circ Cardiovasc Interv*. 2012;5:00-00.)**

Key Words: optical coherence tomography ■ troponin T ■ thin cap fibroatheroma ■ periprocedural myocardial infarction

Periprocedural myocardial infarction (type IVa MI)[1] is caused by procedure-related cell necrosis that occurs after percutaneous coronary intervention (PCI). It is diagnosed when an increase of a marker of cardiac necrosis is observed and remains a frequent complication of PCI, occurring in between 5% and 44% of the procedures.[2,3] Of note, even a small post-PCI biomarker increase is significantly associated with an adverse short- and long-term outcome.[4] Previous studies have used intravascular ultrasound (IVUS) to identify atheroma features associated with type IVa MI, showing both plaque burden[5,6] and necrotic core[7,8] as strong risk factors. Few studies, however, have involved post-PCI evaluation.[5,9] Two recent studies showed time-domain optical coherence tomography (TD-OCT) defined thin-cap fibroatheroma (TCFA) to be associated with type IVa MI[10,11]; these studies, however, were conducted on pre-PCI images only.

We sought to systematically examine frequency-domain (FD)-OCT-defined plaque features, assessed both before and after the procedure, in order to establish their potential impact on type IVa MI, defined as a postprocedural increase of troponin T (TnT) levels.[1]

Received September 10, 2011; accepted December 14, 2011.

From the Department of Cardiovascular Medicine, Policlinico A. Gemelli, Catholic University of the Sacred Heart, Rome, Italy (I.P., L.D.V., F.B., G.N., C.T., A.M.L., L.M.B., R.V., F.C.); U.O.S. di Emodinamica, Ospedale della Misericordia, ASL 9, Grosseto, Italy (U.L.).

Presented in part at the American Heart Association Scientific Sessions, November 2011, Orlando, FL, and published in abstract form (*Circulation.* 2011;124:A12390).

The online-only Data Supplement is available with this article at http://circinterventions.ahajournals.org/lookup/suppl/doi:10.1161/CIRCINTERVENTIONS.111.965624/-/DC1.

Correspondence to Italo Porto, MD, PhD, Department of Cardiovascular Medicine, Policlinico A. Gemelli, Catholic University of the Sacred Heart, Largo Agostino Gemelli 8, 00168 Roma, Italy. E-mail italo.porto@gmail.com

Circ Cardiovasc Interv **is available at http://circinterventions.ahajournals.org** **DOI: 10.1161/CIRCINTERVENTIONS.111.965624**

WHAT IS KNOWN

- Periprocedural (Type IVa) myocardial infarction, which is a frequent complication of percutaneous coronary intervention in stable and unstable patients, has prognostic implications for long-term outcomes.
- Intravascular ultrasound studies suggest that larger plaque volumes with an extensive lipid core in the target lesion are related to an increased risk of periprocedural myocardial infarction.
- Time-domain optical coherence tomography data highlight thin-cap fibrous atheroma as a predictor of periprocedural myocardial infarction.

WHAT THE STUDY ADDS

- Frequency-domain optical coherence tomography, performed both before and after percutaneous coronary intervention, confirms the presence of thin-cap fibrous atheroma and adds intrastent thrombus and intrastent dissection as independent predictors of periprocedural myocardial infarction.
- Tissue prolapse through stent struts not associated with periprocedural myocardial infarction.

Methods

Study Population

Fifty patients presenting with either non-ST elevation MI (NSTEMI) (25 patients) or stable angina (25 patients) were retrospectively extracted from the FD-OCT database of the Department of Cardiovascular Medicine, Policlinico A. Gemelli, Catholic University of the Sacred Heart, Rome, Italy, out of the 151 patients who underwent FD-OCT examination from June 2010 to June 2011. All patients had to undergo PCI with a single-stent implantation for a single, native, de novo coronary lesion. A study flow chart is reported in Figure 1. Patient-related exclusion criteria were PCI for ST elevation MI (STEMI) or multiple PCI during the index procedure. Other exclusion criteria were fever, malignancy, left ventricular ejection fraction <45%, atrial fibrillation, and reduced renal function (creatinine clearance <60 mL/min) because of concerns regarding the specificity of TnT in such patients.[12] All patients received a drug-eluting stent, and none were treated with IIb–IIIa glycoprotein inhibitors. Lesion-related exclusion criteria were left main or aorto-ostial involvement, heavily calcified lesion, tortuous vessel, or angiographic evidence of coronary dissection or side branch occlusion after PCI.

NSTEMI was defined as progressive crescendo pattern or angina at rest, associated with ST segment depression or T-wave inversion on EKG and increased admission TnT (at least >0.03 mg/dL). Stable angina was defined as no change in frequency, duration, or intensity of angina symptoms within 6 weeks before PCI.

Type IVa MI Definition and TnT Assay

Patients were divided into 2 groups, based on TnT-defined type IVa MI. TnT was measured using Roche Diagnostics reagents on an Elecsys 2010 Immunoassay Analyzer. The lower detection limit was 0.01 ng/mL (99th percentile of reference control group). TnT was analyzed at admission, before PCI and at 12 and 24 hours after PCI. Type IVa MI was defined in patients with stable angina (all had undetectable pre-PCI troponin values) as a rise of at least 0.03 mg/dL (>3 times the 99th percentile of the upper reference limit) in post-PCI TnT values.[1] Type IVa MI was defined in NSTEMI as a pre-PCI TnT fall pattern, followed by post-PCI TnT rise of >20% in at least 1 out of 2 post-PCI determinations.[1,13] All patients were

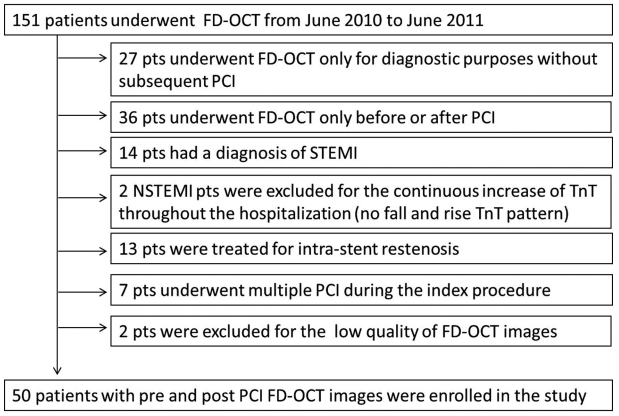

Figure 1. Study flow diagram.

treated with aspirin (100 mg/d), clopidogrel (600-mg loading dose, followed by 75 mg/d), and statins. Patients with NSTEMI were also treated with weight-adjusted low-molecular-weight heparin. The study protocol was approved by the institutional review board, and informed written consent was obtained from each patient.

PCI and FD-OCT Procedures

PCI was performed with a 6Fr guiding catheter in all patients. Unfractionated heparin was administrated during PCI, with a target activated clotting time of >250 seconds. A 0.014-inch guide wire was placed distally in the target vessel, and an intracoronary injection of 200 μg of nitroglycerin was performed. FD-OCT images were acquired with a commercially available system (C7 System; LightLab Imaging Inc/St Jude Medical, Westford, MA) after the OCT catheter (C7 Dragonfly; LightLab Imaging Inc/St Jude Medical, Westford, MA) was advanced to the distal end of the target lesion. The first FD-OCT run was conducted before either direct stent implantation or balloon predilatation (pre-PCI run). The entire length of the region of interest was scanned using the integrated automated pullback device at 20 mm/s. During image acquisition, coronary blood flow was replaced by continuous flushing of contrast media directly from the guiding catheter at a rate of 4 mL/s with a power injector (MEDRAD Avanta®, Siemens, Germany) in order to create a virtually blood-free environment. Twenty-one out of 50 lesions (42%) were predilated with undersized (1.5 or 2 mm) compliant balloons. Stenting was performed using a single drug-eluting-stent implantation. Postdilatation with a noncompliant balloon was performed in 33 out of 50 stents (66%). A second FD-OCT run was subsequently performed (post-PCI run). No FD-OCT related complications occurred.

FD-OCT Image Analysis

All images were recorded digitally, stored, and every single frame (0.2 mm) analyzed by 2 independent investigators (I.P. and L.D.V.), who were blinded to clinical and laboratory data. When there was discordance between the observers, a consensus was obtained. Offline analysis was performed with proprietary software (LightLab Imaging) after confirming proper calibration settings of the Z-offset.

FD-OCT plaque analysis was conducted on pre-PCI runs and was restricted to the vessel segment that was stented on the post-PCI run using fiduciary landmarks (bifurcations, calcium). Plaque analysis was targeted to plaque characterization, ruptured plaque, TCFA (Figure 2A), thrombus,[14,15] and microvessels.[16] When a plaque contained 2 or more lipid-containing quadrants, it was considered a lipid-rich plaque, and lipid arc and cap thickness were measured.[11] TCFA was defined as a lipid-rich plaque with a fibrous cap thickness of ≤65 μm.[15,17] A microchannel was defined as a no-signal tubuloluminal structure without a connection to the vessel lumen recognized on ≥3 consecutive cross-sectional OCT images.[17]

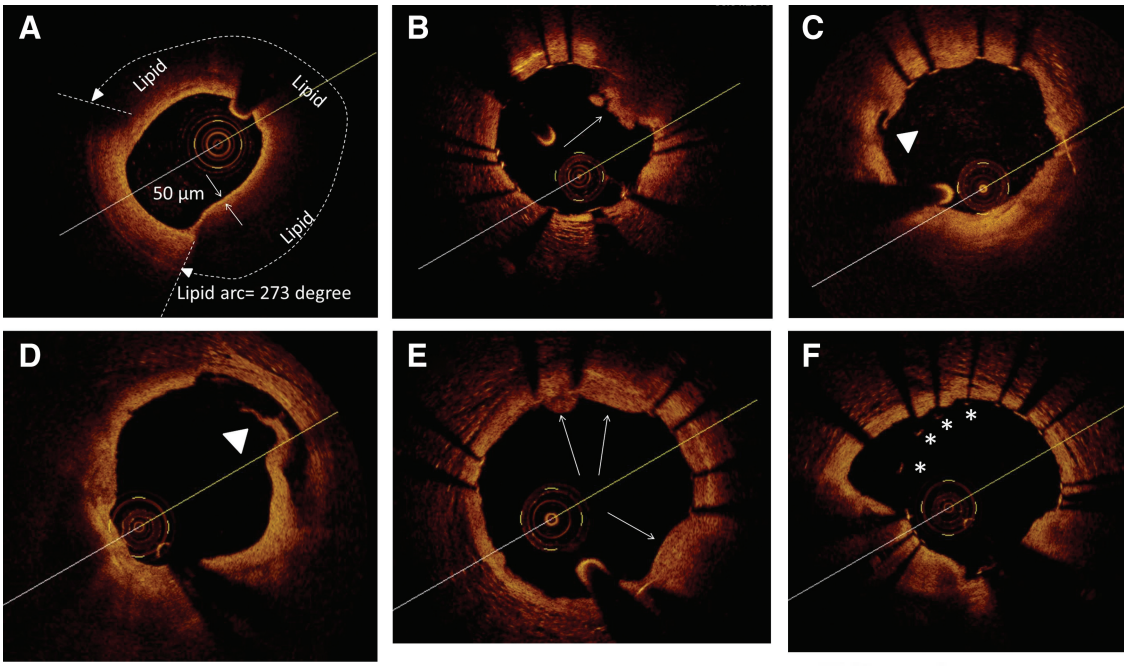

Figure 2. FD-OCT images of main plaque features pre- and post-PCI. **A**, TCFA is imaged. Lipid arc is 273°, and cap thickness at the thinnest portion is 50 μm (arrows). **B**, Intrastent thrombus (arrow) is imaged as an irregular mass with dorsal shadowing protruding within the lumen. Stent struts can be identified from their bright "blooming" appearance and characteristic dorsal shadowing. **C**, Dissection (arrowhead), located in the body of the stent. **D**, Dissection (arrowhead), located at the stent edge. **E**, Tissue prolapse (arrow) is imaged as protrusion of tissue between stent struts extending inside a circular arc, connecting adjacent struts. **F**, Malapposed stent struts are shown (asterisks).

Thrombus was identified as a mass with dorsal shadowing protruding into the vessel lumen or discontinuous from the surface of the vessel wall.[14]

FD-OCT stent analysis was also performed on post-PCI runs and was targeted to intrastent thrombus[18](Figure 2B), intrastent dissection[18] (Figure 2C), edge dissection[17,19] (Figure 2 days), tissue prolapse[18] (Figure 2E), incomplete stent apposition,[20] malapposition length, and number of malapposed struts per cross-section[21] (Figure 2F). Intrastent thrombus was defined as an irregular mass with dorsal shadowing protruding into the lumen or a luminal mass with dorsal shadowing that was not connected to the vessel wall.[18] Intrastent dissection was defined as a disruption of the luminal vessel surface in the stented segment, while edge dissection was a disruption of the luminal vessel surface at stent edges (within 5 mm proximal and distal to the stent, with no visible struts).[18] Tissue prolapse was defined as a convex-shaped protrusion of tissue between adjacent stent struts toward the lumen, without disruption of the continuity of the luminal vessel surface and with a luminal extension of >50 μm.[18] Maximal intraluminal prolapse length was measured as a perpendicular distance from the arc connecting adjacent struts to the greatest extent of protrusion.[18] Prolapse volume (mm^3) was calculated as the sum of tissue prolapse area (mm^2) of each cross-section multiplied by the longitudinal prolapse length (mm). Incomplete stent apposition was defined as a clear separation between at least 1 stent strut and the vessel wall.[20] A malapposed stent strut was identified when this distance was higher than the sum of strut thickness plus abluminal polymer thickness, according to the stent manufacturer's specifications plus a compensation factor of 20 μm to correct for strut blooming.[22] Distances between the endoluminal surface of the strut reflection and the surface of the vessel wall within stent strut shadow were measured[21] (malapposition length).

Quantitative Coronary Angiographic Analysis

Quantitative coronary angiographic analysis was performed with a validated edge detection system (CAAS Version 5.9, Pie Medical Imaging, Maastricht, the Netherlands). The reference vessel diameter, minimal lumen diameter, and lesion length were measured in pre- and post-PCI diastolic frames from orthogonal projections according to validated protocols.[23] Final angiographic result was assessed by Thrombolysis In Myocardial Infarction flow grade.[24]

Statistical Analysis

Statistical analysis was performed using SPSS 17.0 (SPSS, Inc, Chicago, Illinois). Categorical variables are presented as frequencies and analyzed with the Chi^2 test or Fisher exact test. Most continuous variables were not normally distributed as assessed by the Kolmogorov-Smirnov test for normality, and thus were presented as median and interquartile range (IQR), and natural logarithmic transformation was applied to the data to allow the Student t test to be used. Pearson's r correlation coefficient was calculated between cap thickness and tissue prolapse. Multivariate logistic regression was performed to assess the impact of a set of factors on periprocedural MI (dependent variable). Univariate analysis was first performed, and all the variables that exhibited a $P<0.05$ were entered en bloc in the multivariate model, along with age and sex as background variables. Model fit was assessed using the Hosmer-Lemeshow goodness of fit model. Cox and Snell R^2 and Nagelkerke R^2 were used to identify the amount of variation in the dependent variable explained by the model. Intraobserver and interobserver differences were investigated with κ measure of agreement. A probability value <0.05 was considered significant.

Results

Clinical Characteristics and Angiographic Results

Clinical characteristics of the enrolled patients are shown in Table 1.

Type IVa MI was diagnosed in 21 patients, while the other 29 were the control group. The type IVa MI group had a median12-hour post PCI TnT of 0.72 ng/dL (IQR 0.04 to 0.85) that decreased to a median of 0.38 ng/dL (IQR 0.06 to 0.45) at 24-hour post-PCI determination. No patient had

Table 1. Baseline Clinical Characteristics

Baseline Characteristics	All Patients (50)	Type IVa MI (21)	Control (29)	*P* Value
Age, y	65 (60–76)	65 (60–76)	65 (60–71)	0.85
Male gender, n (%)	38 (76)	18 (85.7)	20 (69)	0.17
Hypertension, n (%)	41 (82)	17 (81)	24 (82.8)	1
Hypercholesterolemia, n (%)	36 (72)	16 (76.2)	20 (69)	0.75
Diabetes mellitus, n (%)	17 (34)	6 (28.6)	11 (37.9)	0.55
Current smoker, n (%)	18 (36)	10 (47.6)	8 (27.6)	0.23
Previous PCI, n (%)	18 (36)	8 (38.1)	10 (34.5)	0.79
Previous MI, n (%)	17 (34)	7 (33.3)	10 (34.5)	0.93
NSTEMI, n (%)	25 (50)	12 (57.1)	13 (44.8)	0.56
Statin use, n (%)	50 (100)	21 (100)	29 (100)	1
Beta-blockers, n (%)	38 (76)	17 (81)	21 (72.4)	0.52
ACE-inhibitors, n (%)	28 (56)	9 (42.9)	19 (65.5)	0.15
Aspirin, n (%)	50 (100)	21 (100)	29 (100)	1
Clopidogrel, n (%)	50 (100)	21 (100)	29 (100)	1
Diuretics, n (%)	13 (26)	6 (28.6)	7 (24.1)	0.75
Ejection fraction, %	64 (47–65)	53 (47–64)	60 (50–65)	0.69
Total cholesterol, mg/dl	184 (146–215)	159 (141–200)	191 (154–225)	0.30
LDL, mg/dl	100 (69–133)	91 (62–99)	123 (68–146)	0.08
HDL, mg/dl	41 (36–53)	38 (35–40)	46 (37–53)	0.49
Triglycerides, mg/dl	107 (83–188)	131 (92–242)	89 (83–188)	0.38
Creatinine, mg/dl	1.15 (1–1.37)	1.15 (0.98–1.42)	1.15 (1.00–1.32)	0.43
White blood cells, 10^9/l	7.62 (5.99–9.80)	7.97 (6.66–9.95)	7.15 (5.64–9.74)	0.58
C-reactive protein, mg/l	0 (0–13.3)	0 (0–13.3)	1.9 (0–16.4)	0.90

Values are expressed as median (interquartile range) or absolute number of cases (relative percentage) as appropriate.

significant electrocardiographic changes after PCI, while transient chest pain was observed in 3 patients in the type IVa MI group. In all cases, chest pain subsided after a maximum of 3 hours.

Fifty vessels were analyzed: 22 were Left Anterior Descending, 16 were Left Circumflex, and 12 were Right Coronary Artery. All lesions were successfully treated with stenting: 29 with everolimus-eluting stent (Xience Prime, Abbott) and 21 with zotarolimus-eluting stent (Resolute Integrity, Medtronic). Quantitative coronary angiographic results are shown in Table 2. Minimal lumen diameter, reference vessel diameter, and stenosis percentage were not different between groups at both pre-PCI and post-PCI angiograms. Angiographic thrombus and final Thrombolysis In Myocardial Infarction flow 0 to 2 were not different between groups.

Pre-PCI FD-OCT Findings

FD-OCT results for plaque analysis conducted on pre-PCI runs are shown in Table 3.

TCFA was the only feature significantly associated with type IVa MI (76.2% versus 41.4%; $P=0.017$). In contrast, minimum lumen area, frequency of lipid plaques, lipid plaque cap thickness, and lipid arc angle were not different between groups, but when the number of lipid quadrants was considered, a trend toward a higher number of lipid quadrants was observed in the type IVa MI group. Finally, presence of thrombus and microvessels did not significantly differ between groups.

Post-PCI FD-OCT Findings

FD-OCT results for stent analysis conducted on post-PCI runs are shown in Table 4.

Intrastent thrombus was significantly more frequent in type IVa MI than in the control group (61.9% versus 20.7%; $P=0.04$), as was intrastent dissection (61.9% versus 31%; $P=0.03$). In contrast, tissue prolapse volume, maximal intraluminal prolapse length, incomplete stent apposition, malapposition length, and the number of malapposed struts per cross-section were not significantly different between groups, as was stent edge dissection.

Finally, stented TCFA (n=28) showed greater maximal intraluminal prolapse length compared with non-TCFA (396 μm [IQR 283 to 485] versus 301 μm [IQR 205 to 337.5; $P=0.034$]), while prolapse volume was not different ($P=0.73$).

We were not able to find other significant associations between pre- and post-FD-OCT findings, with the exception of the calculated Pearson correlation coefficient between cap thickness pre-PCI and maximal intraluminal prolapse length on post-PCI images ($R=-0.53$; $P=0.04$).

Predictors of Type IVa MI

The findings of univariate and multivariate logistic regression using type IVa MI as dependent variable are shown in Table 5.

The final multivariate model contained 5 variables (age, male sex, TCFA, intrastent thrombus, and intrastent dissection). The χ^2 value for the Hosmer-Lemeshow test was 6.93,

Table 2. Angiographic Findings

Measure or Variable	All Patients (50)	Type IVa MI (21)	Control (29)	*P* Value
ACC/AHA B2/C lesion, n (%)	38 (76)	17 (81)	21 (72.4)	0.48
Multiple diseased vessels, n (%)	33 (66)	14 (66.7)	19 (65.5)	0.93
Balloon predilatation, n (%)	21 (42)	10 (47.6)	11 (37.9)	0.49
Everolimus-eluting stent, n (%)	29 (58)	14 (66.7)	15 (51.7)	0.29
Zotarolimus-eluting stent, n (%)	21 (42)	7 (33.3)	14 (48.3)	0.29
Stent length, mm	18 (18–28)	20 (15.5–28)	18 (18–29)	0.60
Balloon postdilatation, n (%)	33 (66)	14 (66.7)	19 (65.5)	0.93
Postdilatation pressure, atm	16 (12–18)	15 (12–17)	16 (13.5–20)	0.3
Bifurcated lesion, n (%)	15 (30)	8 (38.1)	7 (24.1)	0.28
Pre-PCI MLD, mm	0.72 (0.52–0.98)	0.70 (0.51–1.01)	0.72 (0.52–0.99)	0.67
Pre-PCI RD, mm	2.66 (2.33–3.09)	2.93 (2.29–3.15)	2.52 (2.34–2.95)	0.71
Pre-PCI % stenosis, %	72.5 (65–78.5)	72 (67–77)	73 (64–79)	0.78
Lesion length, mm	9.39 (7.16–12.8)	10.9 (7.59–13.88)	9.01 (6.81–11.4)	0.79
Thrombus, n (%)	5 (10)	2 (9.5)	3 (10.3)	1
Post-PCI MLD, mm	2.43 (2.18–2.78)	2.64 (2.21–2.71)	2.37 (2.14–2.71)	0.45
Post-PCI RD, mm	2.74 (2.46–3.17)	3.16 (2.64–3.36)	2.67 (2.37–3.07)	0.1
Post-PCI % stenosis, %	13 (6–17)	16 (12–17)	11 (5–14)	0.1
Post-PCI TIMI flow 0–2, n (%)	5 (10)	2 (9.5)	3 (10.3)	1

Values are expressed as median (interquartile range) or absolute number of cases (relative percentage) as appropriate. Minimal luminal diameter (MLD), reference diameter (RD), percentage (%) stenosis before and after PCI were calculated by quantitative coronary angiography (QCA) analysis. Bifurcated lesions were defined as lesions >50% located in a major bifurcation and with a main vessel visual diameter ≥2.5 mm and a side branch visual diameter ≥2.0 mm. Thrombus refers to angiographic evidence of haziness into the culprit vessel.

with a significant level of 0.54. The strongest predictor of type IVa MI was TCFA, followed by intrastent dissection and intrastent thrombus. Moreover, the predictors were not related to each other as suggested by χ^2 analysis of TCFA and intrastent thrombus ($P=0.16$) or TCFA and intrastent dissection ($P=0.69$) and intrastent thrombus and intrastent dissection ($P=0.70$).

Intraobserver and Interobserver Agreement

We tested the degree of agreement for TCFA in pre-PCI runs and for intrastent thrombus in post-PCI runs. Kappa measure of agreement for intraobserver agreement was 0.96 ($P=0.0001$) for TCFA and 0.92 ($P=0.0001$) for intrastent thrombus. Interobserver variability for TCFA and intrastent thrombus was 0.84 ($P=0.0001$) and 0.84 ($P=0.0001$), respectively.

Discussion

Our study identified FD-OCT-defined TCFA, intrastent thrombus, and intrastent dissection as independent predictors of type IVa MI. In contrast, ruptured plaque and plaque

Table 3. FD-OCT Plaque Analysis on Pre-PCI Runs

OCT Features	All Patients (50)	Type IVa MI (21)	Control (29)	*P* Value
MLA, mm^2	2.1 (1.5–3.1)	2.1 (1.5–2.8)	2.1 (1.5–3.2)	0.79
Lipid plaque, n (%)	43 (86)	18 (85.7)	25 (86.2)	1
TCFA, n (%)	28 (56)	16 (76.2)	12 (41.4)	0.017*
Ruptured plaque, n (%)	14 (28)	6 (28.6)	8 (27.6)	1
Thrombus, n (%)	8 (16)	3 (14.3)	5 (17.2)	1
Microvessel presence, n (%)	28 (56)	11 (52.4)	17 (58.6)	0.77
Cap thickness, μm	62 (46–128)	48 (41–111)	65 (52–114)	0.15
Lipid arc, degree	205 (168–228)	225 (198–257)	193 (150–217)	0.54
Lipid quadrants				0.06
0	2 (4)	0	2 (6.9)	
1 (≤90°)	5 (10)	3 (14.3)	2 (6.9)	
2 (>90°; ≤180°)	11 (22)	1 (4.8)	10 (34.5)	
3 (>180°; ≤270°)	27 (54)	15 (71.4)	12 (41.4)	
4 (>270°)	5 (10)	2 (9.5)	3 (10.3)	

Values are expressed as median (interquartile range) or absolute No. of cases (relative percentage) as appropriate. MLA indicates minimum lumen area. * indicates a $P<0.05$.

Table 4. FD-OCT Stent Analysis on Post-PCI Runs

OCT Features	All Patients (50)	Type IVa MI (21)	Control (29)	*P* Value
Imaged stent length, mm	20.2 (17.4–28.3)	22.4 (16.2–29.4)	20.2 (18.7–28.2)	0.7
Maximal intra-luminal prolapse length, μm	343 (272–442)	327 (232–466)	337 (254–426)	0.92
Tissue prolapse volume, mm^3	4.9 (2.5–8.1)	4.5 (2.5–7.7)	4.9 (2.6–8.2)	0.72
Intra-stent thrombus, n (%)	19 (38)	13 (61.9)	6 (20.7)	0.04*
Intra-stent dissection, n (%)	22 (44)	13 (61.9)	9 (31)	0.03*
Edge dissection, n (%)	17 (34)	9 (42.9)	8 (27.6)	0.36
Incomplete stent apposition, n (%)	18 (36)	8 (38.1)	10 (34.5)	1
Malapposition length, μm	339 (201–624)	339 (155–857)	445 (256–572)	0.67
Malapposed struts per cross section, n°	3 (2–3)	3 (2–5)	2 (2–3)	0.08
Total struts per cross section, n°	10 (10–11)	10 (8–11)	10 (10–12)	0.13

Values are expressed as median (interquartile range) or absolute number of cases (relative percentage) as appropriate. * indicates a $P<0.05$.

"prolapse" through stent struts were not significantly associated with type IVa MI.

TCFA is characterized by a necrotic core and a thin fibrous cap[25] and is often associated with positive vessel remodeling,[26] all features of rupture-prone plaque.[27] While the association between the presence of a necrotic core and type IVa MI had previously been ascertained using radiofrequency-based analysis of IVUS images,[28,29] recent studies have shown that OCT-defined TCFA, also when considered in its single components, namely reduced cap thickness[10]and greater number of lipid quadrants,[30] is associated with type IVa MI and/or angiographic slow flow, in both stable[11,27] and unstable patients[30]; however, the previous version of OCT (time-domain) was used in these studies, and the culprit vessel was not imaged after stenting. We were able to broadly confirm the association of TCFA with type IVa MI, and we also found more lipid quadrants (although this difference was not strictly significant) in type IVa MI group, but we failed to find differences for cap thickness. While this discrepancy may be related to our smaller sample size, we, like Tanaka and colleagues,[30] included patients with NSTEMI, who, on average, have a less thick fibrous cap than stable patients (see online-only Supplemental Table 1),[31] thus potentially diluting the effect of a thin cap on type IVa MI. Interestingly, while maximal intraluminal prolapse was higher in patients with an underlying TCFA, it did not predict type IVa MI.

Previous studies from a single Japanese group found an association between prestenting ruptured plaque and type IVa MI assessed by post-PCI creatine kinase-MB (CK-MB).[10,27] While the morphology of these ruptures differed according to the clinical presentation,[31] a very recent study from the same cohort failed to confirm a significant association between ruptured plaque and type IVa MI assessed by troponin I elevation.[11] In our cohort, also, we could not confirm this association using TnT. The reasons for this discrepancy are not clear and might be related to the different sensitivity of troponins versus CK-MB assays in the detection of myocardial damage, as well as to the different prevalence of ruptured plaque in the 2 studies.

The most novel part of our results lies in the identification of intrastent thrombus and intrastent dissection at post stenting FD-OCT analysis as predictors of type IVa MI, as well as in the lack of association with prestenting thrombus, ruptured plaque, and plaque tissue prolapse.

Recently, Lee and colleagues[11] failed to find an association between prestenting thrombus presence and type IVa MI assessed by increased troponin I. Accordingly, Yonetsu and colleagues[10] could not find any relation between prestenting thrombus presence and type IVa MI, as defined by increased CK-MB. We confirmed these data in a cohort of TnT-defined type IVa MI, but we were additionally able to show that post-PCI intrastent thrombus was a good and independent predictor of type IVa MI. Indeed, pre-PCI thrombus may be crushed beneath the stent struts, thus preventing possible embolization. Post-PCI intrastent thrombus, instead, developing on the luminal side of the stent struts, is theoretically able to embolize distally.[32] This notion is in keeping with the idea that increased platelet reactivity is a major risk factor for type

Table 5. Univariate and Multivariate Logistic Regression

	Univariate Logistic Regression			Multivariate Logistic Regression		
	OR	95% CI	*P* Value	OR	95% CI	*P* Value
Age				0.98	0.90–1.06	0.63
Male sex				3.54	0.65–19.19	0.14
TCFA	4.53	1.30–15.77	0.017	29.79	1.36–32.08	0.008
Intra-stent thrombus	6.22	1.77–21.92	0.04	5.55	1.24–24.86	0.025
Intra-stent dissection	3.60	1.10–11.76	0.03	5.33	1.16–24.34	0.031

The model as a whole, explained between 34% (Cox and Snell R^2) and 46% (Nagelkerke R^2) of the variance in type IVa MI, and correctly classified in 80% of cases.

IVa MI.[33] Of note, very recently, a genetic allele linked to limited clopidogrel efficacy has been associated with intrastent thrombus as defined by FD-OCT.[34]

Additionally, we found intrastent dissection as a predictor of type IVa MI, while no association was detected with edge dissection. Recently, Gonzalo and colleagues[18] showed different OCT-defined features between these 2 types of dissection. Intrastent dissection is usually composed of multiple, small intimal tears across the imaged cross-section, while it is of limited longitudinal length. On the other hand, edge dissection is usually a long and single intimal break, extending outside the stent, predicted by the presence of an underlying fibrocalcific or lipid-rich plaque.[19] While we can only indirectly infer on the differential association of these 2 types of dissection with type IVa MI, it is likely that multiple intrastent flaps might work as potential foci for microthrombosis and platelet aggregation.

It must be noted that the specific combination of predictors (TCFA, intrastent thrombus, and intrastent dissection) of type IVa MI in this carefully selected sample is likely to underscore an embolic origin of these periprocedural infarctions. Other mechanisms (such as neurohormonal activation, inflammation, or oxidative stress), however, could not be excluded.[35]

Also interesting in our study is the lack of association between the presence and amount of plaque prolapse and type IVa MI. Prolapse of plaque material on the luminal side of a stent has been previously studied by IVUS and shown to occur in one fourth of infarct-related arteries[9] and in 16% of stable patients with diabetes.[36] It was predicted by plaque rupture and positive remodeling, together with longer stent length[9] and certain stent types.[37] Plaque prolapse volume by IVUS predicted type IVa MI in a sample of patients with acute coronary syndrome.[9] Of note, these studies were all conducted with 20-MhZ IVUS systems, likely to severely underestimate the amount of tissue prolapse because of its low resolution. Moreover, IVUS is not able to differentiate poststenting prolapse from intrastent thrombus, because of their similar echogenicity.[38] With OCT, in contrast, tissue prolapse is observed almost universally after stenting[18,20] and can be readily differentiated from thrombus.[17]

Finally, the overall incidence of type IVa MI in our sample (21/50, 42%), while relatively high, is in line with previous data. Indeed, a >3× upper limits of normal troponin elevation was observed in around 25% of stented patients in Lee's paper,[11] only involving stable patients, and in 47% of a sample similar to ours.[39] Moreover, the high overall incidence (33/50, 66%) of postdilatation with noncompliant balloons, which is common practice in our center, may also explain why it did not predict type IVa MI by itself.

Limitations

Two important limitations of our study lay in the fact that we have defined type IVa MI on the basis of raised TnT only, without measuring CK-MB, and that we have analyzed a mixed population including patients with stable angina and NSTEMI.

The "Universal Definition" of MI highlights troponins instead of CK-MB as the best biomarker to define type IVa MI.[1] Troponin absolute elevation after stenting was strongly correlated with magnetic resonance-defined myocardial necrosis for both patients with stable angina and NSTEMI.[35] In our sample, we showed median TnT values to be as high as 72× the 99th percentile of the upper reference limit at 12 hours post-PCI, and 38× at 24 hours post-PCI. Thus, we can assume that TnT elevations seen in our cohort truly represent the release from myocardial necrotic areas.[36] Moreover, we defined type IVa MI in the NSTEMI group as a fall-and-rise TnT pattern with an increase of >20%, as suggested by a consensus document[1] and a published study.[13]

Another limitation concerns the small size of our sample. While a multicenter registry is mandatory in order to fully evaluate the prognostic role of FD-OCT, our study is a single-center study that has used tight inclusion criteria (such as a single, de novo lesion treated with a single, third-generation drug-eluting stent) and strict exclusion criteria[13]; however, our results have still to be considered as only hypothesis-generating.

Finally, although thrombus tends to have an irregular surface; tissue prolapsed, a smooth border; and dissections, a linear appearance, the final differentiation among these entities remains a potential limitation of OCT.

Conclusions

In conclusion, presence of TCFA at pre-PCI FD-OCT, and of intrastent thrombus and intrastent dissection at post-PCI FD-OCT predict type IVa MI in a contemporary sample of patients treated with second-generation drug-eluting stents. Interestingly, 2 of the 3 predictors of type IVa MI were not apparent at pre-PCI FD-OCT.

Sources of Funding

No external funding sources were used for this study. Dr Di Vito is funded in part by the postgraduate program in Molecular and Cellular Cardiology, Catholic University of the Sacred Heart, Rome, Italy.

References

1. Thygesen K, Alpert JS, White HD, Jaffe AS, Apple FS, Galvani M, Katus HA, Newby LK, Ravkilde J, Chaitman B, Clemmensen PM, Dellborg M, Hod H, Porela P, Underwood R, Bax JJ, Beller GA, Bonow R, Van der Wall EE, Bassand JP, Wijns W, Ferguson TB, Steg PG, Uretsky BF, Williams DO, Armstrong PW, Antman EM, Fox KA, Hamm CW, Ohman EM, Simoons ML, Poole-Wilson PA, Gurfinkel EP, Lopez-Sendon JL, Pais P, Mendis S, Zhu JR, Wallentin LC, Fernandez-Aviles F, Fox KM, Parkhomenko AN, Priori SG, Tendera M, Voipio-Pulkki LM, Vahanian A, Camm AJ, De Caterina R, Dean V, Dickstein K, Filippatos G, Funck-Brentano C, Hellemans I, Kristensen SD, McGregor K, Sechtem U, Silber S, Widimsky P, Zamorano JL, Morais J, Brener S, Harrington R, Morrow D, Lim M, Martinez-Rios MA, Steinhubl S, Levine GN, Gibler WB, Goff D, Tubaro M, Dudek D, Al-Attar N. Universal definition of myocardial infarction. *Circulation*. 2007;116:2634–2653.
2. La Vecchia L, Bedogni F, Finocchi G, Mezzena G, Martini M, Sartori M, Castellani A, Soffiati G, Vincenzi M. Troponin T, troponin I and creatine kinase-MB mass after elective coronary stenting. *Coron Artery Dis*. 1996;7:535–540.
3. Shyu KG, Kuan PL, Cheng JJ, Hung CR. Cardiac troponin T, creatine kinase, and its isoform release after successful percutaneous transluminal coronary angioplasty with or without stenting. *Am Heart J*. 1998;135:862–867.
4. Testa L, Van Gaal WJ, Biondi Zoccai GG, Agostoni P, Latini RA, Bedogni F, Porto I, Banning AP. Myocardial infarction after percutaneous coronary intervention: a meta-analysis of troponin elevation applying the new universal definition. *QJM*. 2009;102:369–378.
5. Porto I, Selvanayagam JB, Van Gaal WJ, Prati F, Cheng A, Channon K, Neubauer S, Banning AP. Plaque volume and occurrence and location of periprocedural myocardial necrosis after percutaneous coronary intervention: insights from delayed-enhancement magnetic resonance imaging, thrombolysis in myocardial infarction myocardial perfusion grade analysis, and intravascular ultrasound. *Circulation*. 2006;114:662–669.

6. Mehran R, Dangas G, Mintz GS, Lansky AJ, Pichard AD, Satler LF, Kent KM, Stone GW, Leon MB. Atherosclerotic plaque burden and CK-MB enzyme elevation after coronary interventions: intravascular ultrasound study of 2256 patients. *Circulation*. 2000;101:604–610.
7. Kawaguchi R, Oshima S, Jingu M, Tsurugaya H, Toyama T, Hoshizaki H, Taniguchi K. Usefulness of virtual histology intravascular ultrasound to predict distal embolization for ST-segment elevation myocardial infarction. *J Am Coll Cardiol*. 2007;50:1641–1646.
8. Lee SY, Mintz GS, Kim SY, Hong YJ, Kim SW, Okabe T, Pichard AD, Satler LF, Kent KM, Suddath WO, Waksman R, Weissman NJ. Attenuated plaque detected by intravascular ultrasound: clinical, angiographic, and morphologic features and post-percutaneous coronary intervention complications in patients with acute coronary syndromes. *JACC Cardiovasc Interv*. 2009;2:65–72.
9. Hong YJ, Jeong MH, Ahn Y, Sim DS, Chung JW, Cho JS, Yoon NS, Yoon HJ, Moon JY, Kim KH, Park HW, Kim JH, Cho JG, Park JC, Kang JC. Plaque prolapse after stent implantation in patients with acute myocardial infarction: an intravascular ultrasound analysis. *JACC Cardiovasc Imaging*. 2008;1:489–497.
10. Yonetsu T, Kakuta T, Lee T, Takahashi K, Yamamoto G, Iesaka Y, Fujiwara H, Isobe M. Impact of plaque morphology on creatine kinase-MB elevation in patients with elective stent implantation. *Int J Cardiol*. 2011;146:80–85.
11. Lee T, Yonetsu T, Koura K, Hishikari K, Murai T, Iwai T, Takagi T, Iesaka Y, Fujiwara H, Isobe M, Kakuta T. Impact of coronary plaque morphology assessed by optical coherence tomography on cardiac troponin elevation in patients with elective stent implantation. *Circ Cardiovasc Interv*. 2011;4:378–386.
12. Li D, Jialal I, Keffer J. Greater frequency of increased cardiac troponin T than increased cardiac troponin I in patients with chronic renal failure. *Clin Chem*. 1996;42:114–115.
13. Mandadi VR, DeVoe MC, Ambrose JA, Prakash AM, Varshneya N, Gould RB, Nguyen TH, Geagea JP, Radojevic JA, Sehhat K, Barua RS. Predictors of troponin elevation after percutaneous coronary intervention. *Am J Cardiol*. 2004;93:747–750.
14. Prati F, Regar E, Mintz GS, Arbustini E, Di Mario C, Jang IK, Akasaka T, Costa M, Guagliumi G, Grube E, Ozaki Y, Pinto F, Serruys PW. Expert review document on methodology, terminology, and clinical applications of optical coherence tomography: physical principles, methodology of image acquisition, and clinical application for assessment of coronary arteries and atherosclerosis. *Eur Heart J*. 2010;31:401–415.
15. Jang IK, Tearney GJ, MacNeill B, Takano M, Moselewski F, Iftima N, Shishkov M, Houser S, Aretz HT, Halpern EF, Bouma BE. In vivo characterization of coronary atherosclerotic plaque by use of optical coherence tomography. *Circulation*. 2005;111:1551–1555.
16. Goto I, Itoh T, Kimura T, Fusazaki T, Matsui H, Sugawara S, Komuro K, Nakamura M. Morphological and quantitative analysis of vascular wall and neointimal hyperplasia after coronary stenting: comparison of bare-metal and sirolimus-eluting stents using optical coherence tomography. *Circ J*. 2011;75:1633–1640.
17. Kitabata H, Tanaka A, Kubo T, Takarada S, Kashiwagi M, Tsujioka H, Ikejima H, Kuroi A, Kataiwa H, Ishibashi K, Komukai K, Tanimoto T, Ino Y, Hirata K, Nakamura N, Mizukoshi M, Imanishi T, Akasaka T. Relation of microchannel structure identified by optical coherence tomography to plaque vulnerability in patients with coronary artery disease. *Am J Cardiol*. 2010;105:1673–1678.
18. Gonzalo N, Serruys PW, Okamura T, Shen ZJ, Onuma Y, Garcia-Garcia HM, Sarno G, Schultz C, van Geuns RJ, Ligthart J, Regar E. Optical coherence tomography assessment of the acute effects of stent implantation on the vessel wall: a systematic quantitative approach. *Heart*. 2009;95:1913–1919.
19. Gonzalo N, Serruys PW, Okamura T, Shen ZJ, Garcia-Garcia HM, Onuma Y, van Geuns RJ, Ligthart J, Regar E. Relation between plaque type and dissections at the edges after stent implantation: An optical coherence tomography study. *Int J Cardiol*. 2011;150:151–155.
20. Bouma BE, Tearney GJ, Yabushita H, Shishkov M, Kauffman CR, DeJoseph Gauthier D, MacNeill BD, Houser SL, Aretz HT, Halpern EF, Jang IK. Evaluation of intracoronary stenting by intravascular optical coherence tomography. *Heart*. 2003;89:317–320.
21. Tanigawa J, Barlis P, Di Mario C. Intravascular optical coherence tomography: optimisation of image acquisition and quantitative assessment of stent strut apposition. *EuroIntervention*. 2007;3:128–136.
22. Guagliumi G, Ikejima H, Sirbu V, Bezerra H, Musumeci G, Lortkipanidze N, Fiocca L, Tahara S, Vassileva A, Matiashvili A, Valsecchi O, Costa M. Impact of drug release kinetics on vascular response to different zotarolimus-eluting stents implanted in patients with long coronary stenoses: the LONGOCT study (Optical Coherence Tomography in Long Lesions). *JACC Cardiovasc Interv*. 2011;4:778–785.
23. Garrone P, Biondi-Zoccai G, Salvetti I, Sina N, Sheiban I, Stella PR, Agostoni P. Quantitative coronary angiography in the current era: principles and applications. *J Interv Cardiol*. 2009;22:527–536.
24. Timi Study Group. The Thrombolysis in Myocardial Infarction (TIMI) trial. Phase I findings. *N Engl J Med*. 1985;312:932–936.
25. Virmani R, Burke AP, Farb A, Kolodgie FD. Pathology of the vulnerable plaque. *J Am Coll Cardiol*. 2006;47:C13–C18.
26. Raffel OC, Merchant FM, Tearney GJ, Chia S, Gauthier DD, Pomerantsev E, Mizuno K, Bouma BE, Jang IK. In vivo association between positive coronary artery remodelling and coronary plaque characteristics assessed by intravascular optical coherence tomography. *Eur Heart J*. 2008;29:1721–1728.
27. Lee T, Kakuta T, Yonetsu T, Takahashi K, Yamamoto G, Iesaka Y, Fujiwara H, Isobe M. Assessment of echo-attenuated plaque by optical coherence tomography and its impact on post-procedural creatine kinase-myocardial band elevation in elective stent implantation. *JACC Cardiovasc Interv*. 2011;4:483–491.
28. Uetani T, Amano T, Ando H, Yokoi K, Arai K, Kato M, Marui N, Nanki M, Matsubara T, Ishii H, Izawa H, Murohara T. The correlation between lipid volume in the target lesion, measured by integrated backscatter intravascular ultrasound, and post-procedural myocardial infarction in patients with elective stent implantation. *Eur Heart J*. 2008;29:1714–1720.
29. Hong YJ, Mintz GS, Kim SW, Lee SY, Okabe T, Pichard AD, Satler LF, Waksman R, Kent KM, Suddath WO, Weissman NJ. Impact of plaque composition on cardiac troponin elevation after percutaneous coronary intervention: an ultrasound analysis. *JACC Cardiovasc Imaging*. 2009;2:458–468.
30. Tanaka A, Imanishi T, Kitabata H, Kubo T, Takarada S, Tanimoto T, Kuroi A, Tsujioka H, Ikejima H, Komukai K, Kataiwa H, Okouchi K, Kashiwaghi M, Ishibashi K, Matsumoto H, Takemoto K, Nakamura N, Hirata K, Mizukoshi M, Akasaka T. Lipid-rich plaque and myocardial perfusion after successful stenting in patients with non-ST-segment elevation acute coronary syndrome: an optical coherence tomography study. *Eur Heart J*. 2009;30:1348–1355.
31. Ino Y, Kubo T, Tanaka A, Kuroi A, Tsujioka H, Ikejima H, Okouchi K, Kashiwagi M, Takarada S, Kitabata H, Tanimoto T, Komukai K, Ishibashi K, Kimura K, Hirata K, Mizukoshi M, Imanishi T, Akasaka T. Difference of culprit lesion morphologies between ST-segment elevation myocardial infarction and non-ST-segment elevation acute coronary syndrome: an optical coherence tomography study. *JACC Cardiovasc Interv*. 2011;4:76–82.
32. Niccoli G, Burzotta F, Galiuto L, Crea F. Myocardial no-reflow in humans. *J Am Coll Cardiol*. 2009;54:281–292.
33. Mangiacapra F, Barbato E, Patti G, Gatto L, Vizzi V, Ricottini E, D'Ambrosio A, Wijns W, Di Sciascio G. Point-of-care assessment of platelet reactivity after clopidogrel to predict myonecrosis in patients undergoing percutaneous coronary intervention. *JACC Cardiovasc Interv*. 2010;3:318–323.
34. Sawada T, Shinke T, Shite J, Honjo T, Haraguchi Y, Nishio R, Shinohara M, Toh R, Ishida T, Kawamori H, Kozuki A, Inoue T, Hariki H, Hirata K. Impact of cytochrome P450 2C19*2 polymorphism on intra-stent thrombus after drug-eluting stent implantation in Japanese patients receiving clopidogrel. *Circ J*. 2010;75:99–105.
35. Herrmann J. Peri-procedural myocardial injury: 2005 update. *Eur Heart J*. 2005;26:2493–2519.
36. Futamatsu H, Sabate M, Angiolillo DJ, Jimenez-Quevedo P, Corros C, Morikawa-Futamatsu K, Alfonso F, Jiang J, Cervinka P, Hernandez-Antolin R, Macaya C, Bass TA, Costa MA. Characterization of plaque prolapse after drug-eluting stent implantation in diabetic patients: a three-dimensional volumetric intravascular ultrasound outcome study. *J Am Coll Cardiol*. 2006;48:1139–1145.
37. Shen ZJ, Brugaletta S, Garcia-Garcia HM, Ligthart J, Gomez-Lara J, Diletti R, Sarno G, Witberg K, Serruys PW. Comparison of plaque prolapse in consecutive patients treated with Xience V and Taxus Liberte stents. *Int J Cardiovasc Imaging*. 2010 Dec 21. [Epub ahead of print].
38. Jang IK. Optical coherence tomography or intravascular ultrasound? *JACC Cardiovasc Interv*. 2011;4:492–494.
39. Locca D, Bucciarelli-Ducci C, Ferrante G, La Manna A, Keenan NG, Grasso A, Barlis P, Del Furia F, Prasad SK, Kaski JC, Pennell DJ, Di Mario C. New universal definition of myocardial infarction applicable after complex percutaneous coronary interventions? *JACC Cardiovasc Interv*. 2010;3:950–958.

SUPPLEMENTAL MATERIAL

Expanded Methods and Results

TnT values in NSTEMI and SA patients

NSTEMI group had a median admission TnT of 0.75 ng/dl (IQR 0.08-0.89), a median pre-PCI TnT of 0.52 ng/dl (IQR 0.03-0.77). TnT increased at 12-hour post PCI reaching a median of 0.71 ng/dl (IQR 0.24-0.95) and subsequently decreased at 24-hour post PCI to 0.42 ng/dl (IQR 0.15-0.67). All SA patients had both admission and pre-PCI TnT values below 0.01 ng/dl. SA group had a median 12-h post PCI TnT of 0.12ng/dl (IQR 0.06-0.31) and a median 24-hour post-PCI TnT of 0.75ng/dl (IQR 0.21-1.01).

FD-OCT findings between NSTEMI and SA patients

We performed a subanalysis focused on the FD-OCT differences between NSTEMI and SA patients. Pre-PCI FD-OCT findings are shown in Supplemental Table 1. NSTEMI patients had a greater prevalence of ruptured plaque and thrombus compared with SA patients (48% vs 8%, p=0.002 and 32% vs 0%, p=0.002; respectively). We failed to find differences in terms of either TCFA or lipid plaque.

Post-PCI FD-OCT findings are shown in Supplemental Table 2. NSTEMI patients showed greater prolapse volume compared to SA [6.7mm^3(IQR 3.7-9.9) vs 3.6 mm^3 (IQR 2.1-7.2; p=0.05)], while maximal intra-luminal prolapse length was similar between the two groups [345µm (IQR 269-456) vs 341µm (IQR 290-431; p=0.5)]. Intra-stent dissection was more frequently imaged in SA patients (p=0.004).

Influence of additional FD-OCT pullbacks on post-dilation

All enrolled patients underwent FD-OCT before PCI (*pre-PCI pullback*) and at the end of the procedure (*post-PCI pullback*). However, 23 out of 50 patients (46%) underwent at least one additional FD-OCT (*additional pullback*) before *post-PCI pullback* and 13 of them (26%) were post-dilated with oversized balloons after the additional run, generally based on *additional pullback* findings. These choices were made by the operators. Post-dilatation based on *additional pullback* data was equally distributed between type IVa MI and control groups (6/21 or 28.6% vs 7/29 or 24.1%; p=0.72), as was post-dilatation based on angiographic features only (8/21 or 38.1% vs 12/29 or 41.4%, p=0.8). This was in a context of liberal use of postdilatation with noncompliant balloons (33/50 pts, 66%), reflecting our current practice. We were, however, unable to ascertain any impact of postdilatation (based or not on FD-OCT findings) on type IVa MI in our cohort.

The Supplemental Figure shows how additional FD-OCT pullbacks and postdilatation were distributed in the entire study population.

Association between angiographic final TIMI flow 1-2 and OCT-defined predictors of type IVa MI.

Final TIMI flow 1-2 was rarely observed in the entire population (10%) with no statistical differences between type IVa MI and control groups (9.5% vs 10.3%, p=1).

TCFA, intra-stent thrombus and intra-stent dissection were not statistically different between patients with or without final TIMI flow 1-2 **(**Supplemental Table 3).

Supplemental Table 1. FD-OCT pre-PCI findings between NSTEMI and SA

OCT features	All patients (50)	NSTEMI (25)	SA (25)	p
MLA, mm^2	2.1 (1.5-3.1)	2.1 (1.4-3.4)	2.5 (1.5-3)	0.87
Lipid plaque, n (%)	43 (86)	23 (92)	20 (80)	0.22
TCFA, n (%)	28 (56)	16 (64)	12 (48)	0.25
Ruptured plaque, n (%)	14 (28)	12 (48)	2 (8)	0.002*
Thrombus, n (%)	8 (16)	8 (32)	0	0.002*
Microvessels presence, n (%)	28 (56)	15 (60)	13 (52)	0.56
Cap thickness, µm	62 (46-128)	56 (46-111)	65 (49-143)	0.42
Lipid arc, degree	205 (168-228)	203 (177-239)	208 (132-226)	0.96
Lipid quadrants				0.58
0	2 (4)	0	2 (8)	
1 (≤90°)	5 (10)	2 (8)	3 (12)	
2 (>90°;≤180°)	11 (22)	5 (20)	6 (24)	
3 (>180°;≤270°)	27 (54)	15 (60)	12 (48)	
4 (>270°)	5 (10)	3 (12)	2 (8)	

Values are expressed as median (interquartile range) or absolute number of cases (relative percentage) as appropriate. * indicates a $p< 0.05$.

Supplemental Table 2. FD-OCT post-PCI findings between NSTEMI and SA

OCT features	All patients (50)	Type IVa MI (25)	Control (25)	p
Imaged stent length, mm	20.2 (17.4-28.3)	19 (16.8-27.8)	20.4 (19-29.6)	0.28
Maximal intra-luminal prolapse length, µm	343 (272-442)	345 (269-456)	341 (290-431)	0.5
Tissue prolapse volume, mm^3	4.9 (2.5-8.1)	6.7 (3.7-9.9)	3.6 (2.1-7.2)	0.05
Intra-stent thrombus, n (%)	19 (38)	10 (40)	9 (36)	0.77
Intra-stent dissection, n (%)	22 (44)	6 (24)	16 (64)	0.004*
Edge dissection, n (%)	17 (34)	8 (32)	9 (36)	0.76
Incomplete stent apposition, n (%)	18 (36)	10 (40)	8 (32)	0.55
Malapposition length, µm	339 (201-624)	300 (174-657)	368 (249-677)	0.67
Malapposed struts per cross section, n°	3 (2-3)	3 (2-3)	2 (2-4)	0.73
Total struts per cross section, n°	10 (10-11)	10 (8-11)	10 (10-12)	0.13

Values are expressed as median (interquartile range) or absolute number of cases (relative percentage) as appropriate. * indicates a $p< 0.05$.

Supplemental Table 3. OCT-defined predictors of type IVa MI and final TIMI flow

	TIMI flow 1-2 (5)	TIMI flow 3 (45)	p
TCFA, n (%)	3 (60)	25 (55)	0.84
Intra-stent thrombus, n (%)	1 (20)	18 (40)	0.38
Intra-stent dissection, n (%)	1 (20)	21 (46)	0.25

Supplemental Figure. Flow-chart describing FD-OCT pullbacks

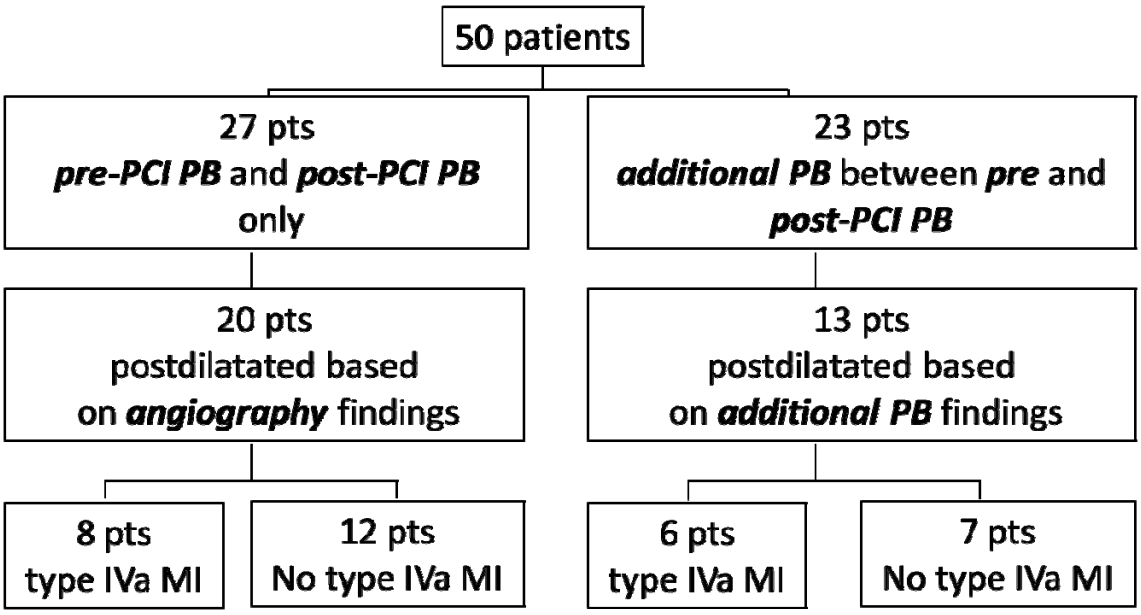

PB refers to pullback.